Hodgkin-Huxley Type Modeling

by

Dylan O'Connell

A Project Report

Submitted to the Faculty

of the

WORCESTER POLYTECHNIC INSTITUTE

In partial fulfillment of the requirements for the

Degree of Master of Science

in

Applied Mathematics

by

April 2014

APPROVED:

_____

Professor Sarah D. Olson, Project Advisor

Abstract

A Hodgkin-Huxley style system of ODEs was developed to model the ion channel activity of A. punctulata sperm flagellum during exposure to resact during chemotaxis. Empirical data was used in conjunction with parameter estimation methods in an attempt for the model to reproduce realistic Voltage potentials and ion concentrations. The change in calcium concentration is of particular interest, as it is essential in the waveform of the flagellum during chemotaxis.

Contents

1 Introduction **7**

1.1 Sperm 7

1.2 Chemotaxis 7

1.3 Cell Membrane 10

2 Hodgkin- Huxley Background **12**

2.1 Nerve Action Potential 12

2.2 Hodgkin-Huxley Type Model 12

2.3 Steady State of Gating Variables 15

3 The Model **16**

3.1 Ion Channels 17

3.2 ODE System 17

3.3 Current Equations 18

3.4 Parameters 20

4 Units and Calculated Constants **21**

4.1 Cell Volume and Surface Area 21

4.2 Calculating cGMP per cell 22

4.3 Cell Capacitance 22

4.4 Determining Ion Flux through Channels from the Faraday Constant and Cell Volume 22

5 Parameter Estimation **24**

5.1 Steady State Case 24

5.2 Testing the Steady State Parameters in the Presence of Resact 26

5.3 Active Case (Resact Present) Parameter Estimation 27

6 Discussion **31**

List of Figures

1 Diagram of sperm. 7

2 Schematic of sperm chemotaxis. 8

3 Experiments: calcium and path curvature of swimming. 9

4 Schematic of channels in Resact mediated chemotaxis pathway. . . 10

5 Membrane Voltage During Resact Stimulation 11

6 Circuit equivalent. 12

7 Behavior of gating. 14

8 Voltage and calcium data in response to varying resact concentrations. 16

9 Steady state parameter estimation, currents. 25

10 Steady state parameter estimation, concentrations. 26

11 Optimal steady state parameter estimation, currents. 27

12 Optimal stead state parameter estimation, concentrations. 28

13 Active (with cGMP) optimized steady state parameters, currents. . 29

14 Active (with cGMP) optimized steady state parameters, concentration. 29

15 Parameter Estimation using Real data for Calcium and Voltage in 25pM of Resact. 30

List of Tables

1 Parameter Values for the model. 20

1 Introduction

1.1 Sperm

In the process of sexual reproduction a male gamete must come into contact with a female gamete. Typically, male gametes are motile whilst the female gametes are not. Male gametes which are motile are referred to as spermatozoon, or simply sperm, and complimentary female gametes are often referred to as eggs. Sperm are composed of a head, which is responsible for carrying the genetic ma-

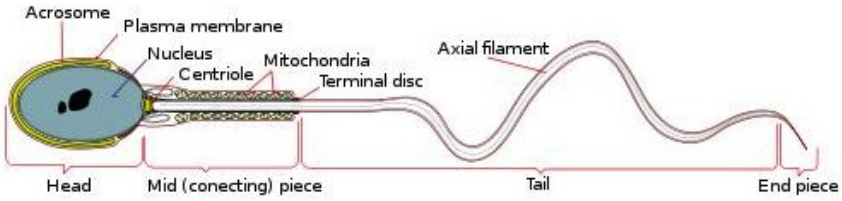

Figure 1: Diagram of sperm, the tail and end piece are known as the flagellum, and are responsible for the movement of the sperm cell. [22].

terial needed for fertilization, a mid piece, and a tail or flagellum responsible for propelling the sperm. A diagram of a sperm is shown in Fig.1.

The sperm which we are interested in, are that of Arbacia punctulata, commonly known as the purple-spined sea urchin. A. punctulata sperm are heavily studied, with a lot of experimental data [10]. As they are similar to human sperm, research and models based on A. punctulata may be useful in further understanding human sperm [20].

1.2 Chemotaxis

Chemotaxis is the movement of an organism based on chemical concentrations in the environment. For A. punctulata sperm, Resact, a protein released by

the egg, is a chemoattractant [9, 10]. This means that the sperm wants to travel along the increasing Resact gradient, which would lead to the source, the egg. Resact binds to receptors on the flagellum and stimulates a signal pathway which excites the sperm and causes it to travel in the direction of increasing Resact. In

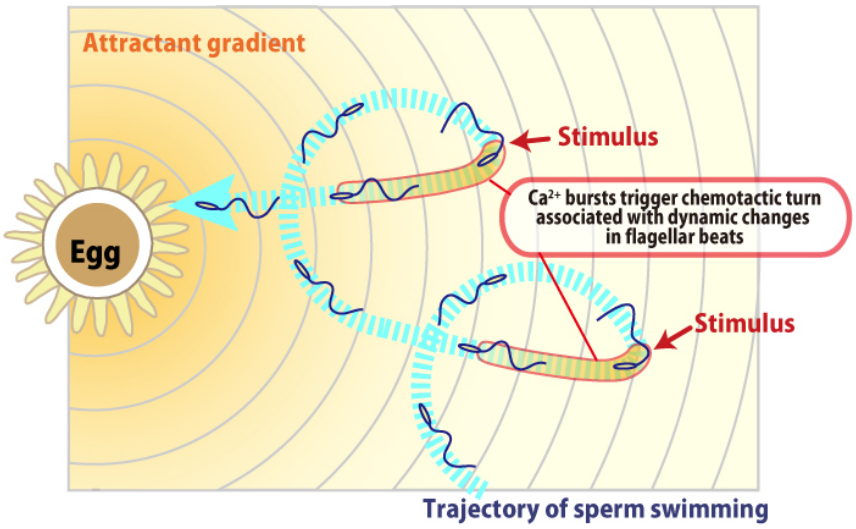

Figure 2: Schematic of sperm chemotaxis, the sperm make sharp turns in accordance with the Resact gradient while following a circular path towards the egg. [13].

Fig.2 it can be seen that the changing Resact concentration causes an intracellular calcium (Ca^{2+}) burst via the signaling pathway along the flagellum. The dynamics of Ca^{2+} oscillations in sea urchin sperm are well documented, see [23, 24, 25]. These Ca^{2+} bursts reorient the sperm in the direction of the egg. It is by this same mechanism that human sperm reorient [21, 19]. The change in intracellular calcium levels cause asymmetrical beat patterns which affect the curvature of the sperms path, allowing for reorientation, as seen in Fig. 3. In Fig. 3A, Ca^{2+} fluorescence and path curvature are shown, in Fig. 3B the black arrow shows where Resact is introduced and the actual path of the sperm. The blue dots on the path in Fig. 3B correspond to the blue dots on the graph of Fig. 3A in order to show

the relation between Ca^{2+} and the path of the sperm.

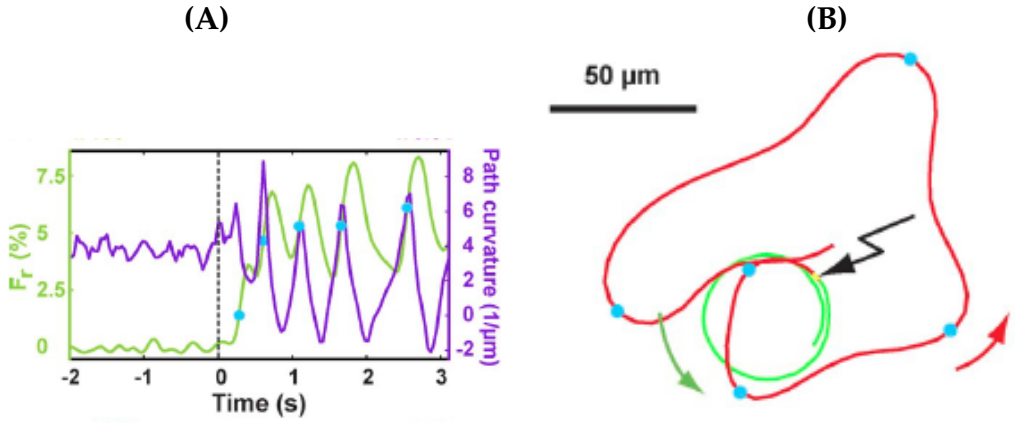

Figure 3: Experiments: calcium and path curvature of swimming. As the calcium levels rise and oscillate, the path curvature follows in a out of phase oscillation. Resact is introduced at time zero in (A), and at the black arrow in (B). The blue dots correlate to show the relation between calcium and curvature of the sperm path. [2].

1.3 Cell Membrane

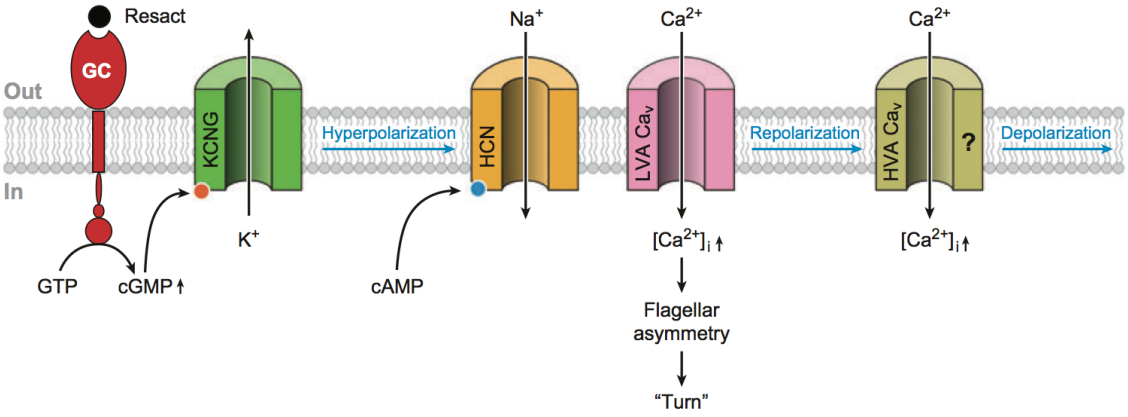

Figure 4: Schematic of channels in Resact mediated chemotaxis pathway. Not included is an exchanger channel to regulate intracellular ion concentrations. [10]

The signaling pathway, shown in Fig.4, is responsible for influx of ca^{2+} and a change in flagellum waveform during chemotaxis. The pathway begins when Resact binds to the gyanylyl cyclase (GC) receptor. This in turn causes the synthesis of cyclic guanosine monophyosphate (cGMP).The production of cGMP then causes the potassium (K^+)-selective nucleotide-gated (KCNG) channels to open [10]. Once these channels are open, K^+ ions flood out the flagellum and cause a hyperpolorization of the cell, meaning the positive charge from the efflux of K^+ ions causes the membrane potential to drop from approximately -42mV to -80mV [17].

The hyperpolarization-actived cyclic nucleotide gated channels (HCN) immediately open and begin to allow sodium (Na^+) into the cell [15]. This begins the depolarization process, as positive Na^+ ions flow into the cell, causing the membrane potential to increase.

The depolarization of the cell causes both the high and low voltage calcium channels (HCA, LVA) to open and allow an influx of ca^{2+}, this causes the voltage

of the membrane to fully depolarize, often rising above the resting potential of -42mV to reach a peak and then slowly refract back to the resting membrane potential [10]. The behavior of the voltage during the signaling process is shown

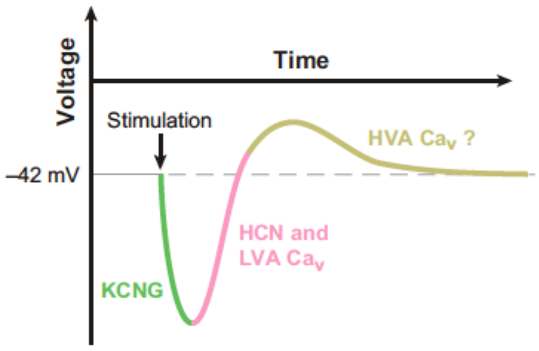

Figure 5: Membrane Voltage During Resact Stimulation, the opening and closing of the ion channels hyperpolarizing and then depolarizing the cell. Channels are labeled in accordance with the part of the voltage curve they are responsible for. [10].

in Fig. 5. Where the stimulation is Resact given to start the signal pathway.

Not pictured in Fig. 4 is an exchanger ion channel, which helps to remove excess intracellular ions in exchange for others. This helps the balance the intracellular ion concentration. Our model uses a NCKX exchanger, which intakes four Na^+ ions while it expels one Ca^{2+} and one K^+ ion. The exchanger ion currents depend linearly on the Ca^{2+} and K^+ intracellular concentrations. So the more internal Ca^{2+} and K^+, the more the exchanger works to evacuate those ions [1] .

2 Hodgkin- Huxley Background

2.1 Nerve Action Potential

Alan Lloyd Hodgkin and Andrew Huxley received the 1963 Nobel Prize for their work in modeling the action potential of the squid giant axon. Nerve action potentials are propagated by the coordinated opening and closing of ion channels along the cell membrane of the axon, due to charge from separation of axons [6].

2.2 Hodgkin-Huxley Type Model

Hodgkin and Huxley treated the cell membrane of the axon as a simple circuit, as the behavior of the biological components, in regards to their electrical properties, behaved as such. The circuit equivalent to a nerve cell is shown in Fig.6.

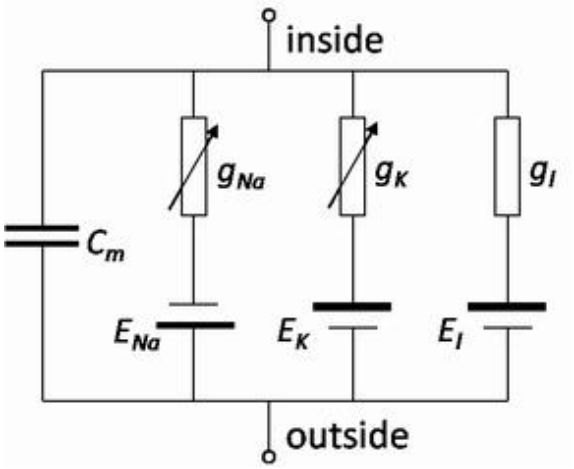

Figure 6: Circuit equivalent of nerve axon. The cell membrane is represented by the capacitor C_m, and the three ion channels, sodium (Na), potassium (K), and the leak channel (l). [12].

The ion channels behave as resistors, and the lipid bilayer of the cell membrane separates ion concentrations, and therefore acts as a capacitor. In order to

observe how voltage changes with time, one must first determine all of the currents. Using standard equations for a circuit, and defining the movement of ions from inside the cell to outside as positive current, we have that the membrane capacitance C_m is

$$C_m = \frac{Q}{V_m}$$

where Q is charge and V_m is the membrane voltage. Current through a capacitor is given by

$$I_c = \frac{dQ}{dt} = C_m \frac{dV_m}{dt}.$$

Now, for each of the ion channels, letting the subscript i denote the i-th channel, assuming the ion channels follow Ohms Law, $V = IR$, we have that

$$I_i = \frac{1}{R_i} V_i.$$

As ion flow is determined by electrical current and the concentration differences across the membrane, we must account for the Nernst potential E_i, which is is the potential that opposes net diffusion of a particular ion through the cell membrane. The Nernst Potential is based on a particular ions concentration on either side of the membrane.

$$I_i = \frac{1}{R_i} \left(V_i - E_i \right).$$

Now, as these channels switch on an off we add a gating variable n which is a value ranging from 0 to 1, we also repalce $\frac{1}{R_i}$ with g_i wich is the maximal conductance (inverse of resistance) for that particular ion channel. Therefore our final equation for the i-th ion channel is:

$$I_i = g_i n_i^{p_i} \left(V_i - E_i \right),$$

where p_i is a power often represeting the number of gates in a channel and the behavior of n is governed by the ODE

$$\frac{dn_i}{dt} = \alpha_{n_i}(1 - n_i) - \beta_{n_i}(n_i),$$

which is described in Fig 7. Now, from Kirchhoff's current law, the sum of our

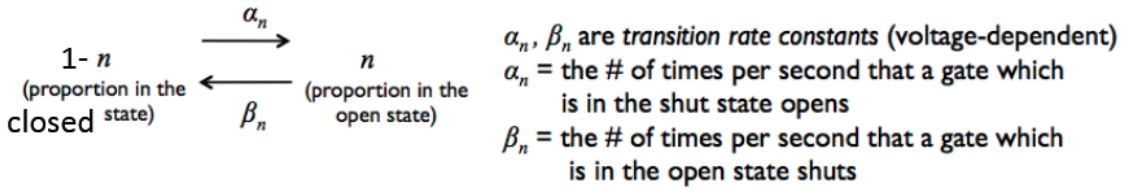

Figure 7: Behavior of gating variable, α_n is the transition rate from closed to open, β_n is the transition rate from open to closed [11].

currents must be zero

$$I_c + \sum_i I_i = 0$$

$$I_c = -\sum_i I_I$$

$$C_m \frac{dV_m}{dt} = -\sum_i I_i$$

Therfore, the change in potential across the membrane is then given by the system

$$\frac{dV_m}{dt} = -\frac{1}{C_m}\sum_i I_i$$

$$I_i = g_i n_i^{p_i} (V_i - E_i)$$

$$\frac{dn_i}{dt} = \alpha_{n_i}(1 - n_i) - \beta_{n_i}(n_i)$$

2.3 Steady State of Gating Variables

The steady state of the gating variables is not only part of the explicit solution for the gating variable equation, but it can also be used to simplify a model which has channels that reach a steady state quickly. This makes an ODE describing the gating behavior unnecessary. Starting with our ODE for n:

$$\frac{dn}{dt} = \alpha_n(1-n) - \beta_n(n)$$

At steady state, we have

$$0 = \alpha_n(1-n_\infty) - \beta_n(n_\infty)$$

$$0 = \alpha_n - \alpha_n n_\infty - \beta_n n_\infty$$

$$0 = \alpha_n + (-\alpha_n - \beta_n)n_\infty$$

$$n_\infty = \frac{\alpha_n}{\alpha_n + \beta_n}$$

Now, back to our original ODE for n, one will find that solving the ODE by separation of variables will lead to the solution

$$n = n_\infty - (n_\infty - n_0)e^{-\frac{t}{\tau}}$$

where

$$\tau = \frac{1}{\alpha_n + \beta_n}.$$

Later in our paper, we will assume some channels reach steady state quickly, and therefore we will replace the gating variable with a function similar to the above solution for n. This can be see in equations (8) and (9).

3 The Model

Our model uses a Hodgkin-Huxley system of ODEs to model the ion channels along the flagellum and intracellular ion concentrations. Initial intracellular ion concentrations, needed for our ODEs and for the estimation of steady state parameters, are from [1]. In order to model the KCNG hyperpolarization directly from Resact, interpolated cGMP data from exposure to Resact was taken from [4, 10]. Lastly, in order to estimate parameters for the active state where the model was subjected to Resact, interpolated voltage and calcium data from [17], seen in in Fig.8 were used. The following system of ODEs was solved in MATLAB by

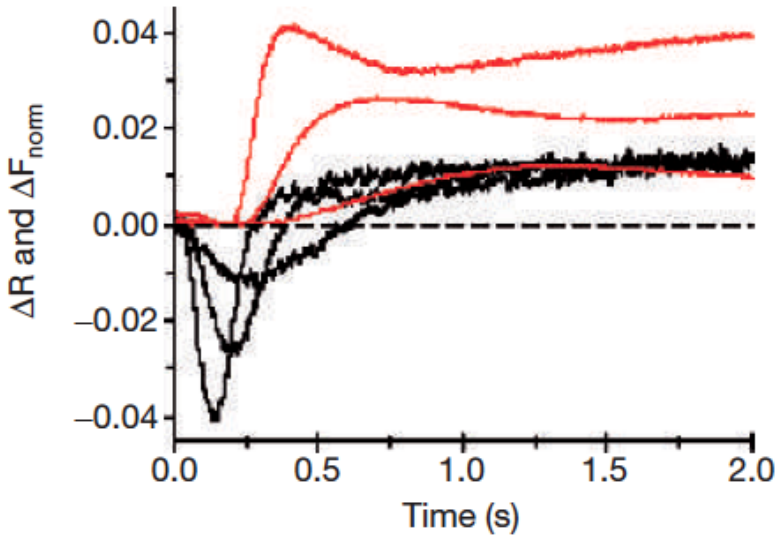

Figure 8: Voltage (Black) and Calcium (Red) Data in response to varying Resact Concentrations. This data was used to estimate parameters for our model when not in a steady state [17].

ode15s.

3.1 Ion Channels

For our model, we have chosen to model the KCNG, HCN, HVA, NCKX exchanger, and a leak channel. Clearly we did not include an LVA channel, this was for simplicity, and was following in the form of the model from [1] where both channels were lumped into one. However, DNA fragments of both HVA and LVA channels have been found in A. punctulata [10].

For our exchanger we chose an NCKX exchanger, as they have been found and localized to A. punctulata flagellum. However NCX exchangers may also play a role in the signal pathway. NCX exchangers have been found in rat sperm flagella, though their existence has not been documented in sea urchin sperm [18]. So to keep the model simple, we will only include a NCKX channel.

It is also worth noting the PCMA channel acts as a pump to remove Ca^{2+}. It has been shown in [8] to be localized in flagella in S. purpuratus, but not A. punctulata. However, both S. purpuratus and A. punctulata had NCKX exchangers, so we reason that for a general sea urchin sperm model NCKX is the dominant Ca^{2+} extrusion mechanism.

3.2 ODE System

The following equations are the proposed model to govern membrane potential and intracellular ion concentrations.

$$\frac{dV_m}{dt} = \frac{-1}{C_m} * (I_{KCNG} + I_{HCN} + I_{HVA} + I_{Leak} + I_{Knckx} + I_{Canckx} + I_{Nanckx}) \quad (1)$$

$$\frac{d[Ca^{2+}]}{dt} = \frac{-1}{2f} * (I_{HVA} + I_{Canckx}) \quad (2)$$

$$\frac{d[Na^{+}]}{dt} = \frac{-1}{f} * (I_{HCN} + I_{Nanckx}) \quad (3)$$

$$\frac{d[K^+]}{dt} = \frac{-1}{f} * (I_{KCNG} + I_{Knckx}) \tag{4}$$

$$\frac{dm}{dt} = m_{\text{inf}} - m \tag{5}$$

where m_{inf} is:

$$m_{\text{inf}} = \frac{1}{1 + \exp\left(\frac{V - V_{KCNG}}{s_{KCNG}}\right)} * \left(\frac{[cGMP]}{K + [cGMP]}\right) \tag{6}$$

The first differential equation, equation (1) is a standard Hodgkin-Huxley Model, where the change in voltage over time is equal to the sum of the ion currents (I_i) from each channel, divided by the capacitance (C_m).

Equations (2)-(4) model the ion flux through the membrane, or their change in concentration in micromolar (μM). Their ion current contributions divided by a product of the cell volume and Faraday constant yield an ion concentration.

The last differential equation (5) is the gating variable for the KCNG channel. While realistically all of the ion channel equations should have an ODE to represent their gating variables, we assume most reach steady state very quickly. However, the gating for the KCNG channel is directly related to cGMP concentrations and we have real cGMP data. We have chosen to let the standard Hodgkin-Huxley gating variable ODE for a gating variable depend on cGMP concentrations and K, in equation (6), where K is a half maximal cGMP concentration.

3.3 Current Equations

Details for the currents from equation (1) are now given for each ion channel.

$$I_{KCNG} = \bar{g}_{KCNG} * m^1 * (V_m - E_{KCNG}) \tag{7}$$

$$I_{HCN} = \bar{g}_{HCN} * (V_m - E_{HCN}) * \frac{1}{1 + \exp\left(\frac{V - V_{HCN}}{s_{HCN}}\right)} \tag{8}$$

$$I_{HVA} = \bar{g}_{HVA} * (V_m - E_{HVA}) * \frac{1}{1 + \exp\left(\frac{V - V_{HVA}}{s_{HVA}}\right)} \tag{9}$$

$$I_{Leak} = \bar{g}_{Leak} * (V_m - E_{Leak}) \tag{10}$$

$$I_{Canckx} = 2 * f * ef * [Ca] * [K] \tag{11}$$

$$I_{Nanckx} = -4 * f * ef * [Ca] * [K] \tag{12}$$

$$I_{Knckx} = f * ef * [Ca] * [K] \tag{13}$$

Equations (7)-(9) are for the current for the KCNG, HCN, and HVA channels, respectively. These are Hodgkin Huxley equations for ion channels,equations (8) and (9) are multiplied by a steady state gating variable term. Equation (10) accounts for the leakage of ions from the membrane, a standard Hodgkin-Huxley practice. Equations (11)-(13) are to describe the NCKX exchanger. The NCKX exchanger uptakes four Na^+ ions while it expels one Ca^{2+} and one K^+ ion. It was assumed that Na^+, Ca^{2+} and K^+ depend linearly on Ca^{2+} and K^+ concentrations [1]. These equations multiply the $[Ca^{2+}]$ and $[K^+]$ concentrations by f to convert them to a current, this current is then multiplied by the flow rate ef and by the number of valence ions passing through the channel.

It is important to note that the Nerst Potential (E_i) component of equations (7)-(10) is dependent on intracellular and extracellular ion concentrations. Letting the subscript i denote the ion/ ion channel.

$$E_i = \frac{RT}{zF} * \left\{ \frac{\text{ion in}_i}{\text{ion out}_i} \right\}$$

These varying Nerst potentials are easily calculated as we have ODEs to calculate

intracellular concentrations and extracellular concentrations can be assumed to be constant. However, in preliminary development of the model, the variance of the E_i's was insignificant given the inner and outer ion conditions given from [1]. As varying Nerst potentials just resulted in noisy currents with little variation, they were left as constant values.

3.4 Parameters

Table 1: Parameter Values for the model.

Parameters	**Value (Lit Value)**
E_{KCNG} (Reversal potential for KCNG, mV)	-80 (-80 in [5])
E_{HCN} (Reversal potential for HCN, mV)	-45 (-30 in [7])
E_{HVA} (Reversal potential for HVA, mV)	19.036397, Estimated (22-29 in [16])
E_{Leak} (Reversal potential for Leak, mV)	-13.771565, Estimated (-50 [3])
g_{KCNG} (max conductance for KCNG, nS)	0.11 (0.04-0.129 in [5])
g_{HCN} (max conductance for HCN, nS)	0.036, Estimated (0.031, 0.043 in [14])
g_{HVA} (max conductance for HVA, nS)	6.8533×10^{-4}, Estimated (0.007 [1])
g_{Leak} (max conductance for Leak, nS)	3×10^{-4}, Estimated (100 in [3])
V_{KCNG} (gating variable for KCNG, mV)	-60 (-25 in [4])
V_{HCN} (gating variable for HCN, mV)	-55 (-45 to -65 in [4])
V_{HVA} (gating variable for HVA, mV)	-16.045268, Estimated (-13 in [1, 16])
s_{KCNG} (step width for KCNG, mV)	10, Estimated
s_{HCN} (step width for HCN, mV)	-15 (-15 in [4])
s_{HVA} (step width for HVA, mV)	-8.8 (8-13 in [16])
e_f (rate of flow through NCKX, $\mu M/ms$ need to check!)	6.1248×10^{-8}, Estimated
C_m (membrane capacitance, pF)	2.8 (Calculated in §4.3)
vol (volume of sperm flagellum, L)	1.413716×10^{-13}
SA (surface area of sperm flagellum, cm^2	2.82×10^{-6}
f ($vol\times$Faraday constant, ms PA μM^{-1})	13.640302

4 Units and Calculated Constants

Preffered Units

- Voltage: mV (millivolts)
- Time: ms (milliseconds)
- Concentration: μM (micromolar)
- Current: pA (picoamps)
- Cunductance: nS (nanosiemens)

4.1 Cell Volume and Surface Area

For a simple approximation, the cell is assumed to be a cylinder with a radius of 1 micron and a length of 45 microns, the end caps of the cylinder are ignored.

Cell volume in m^3 using $r^2 * \pi * h$:

$$(1 \times 10^{-6}\,\mathrm{m})^2 * \pi * (45 \times 10^{-6}\,\mathrm{m}) = 1.41 \times 10^{-16}\,\mathrm{m}^3$$

Converting to liters:

$$1.41 \times 10^{-16}\,\cancel{\mathrm{m}^3} * \frac{1 \times 10^{3}\,\mathrm{L}}{\cancel{\mathrm{m}^3}} = 1.41 \times 10^{-13}\,\mathrm{L}$$

Surface area in cm^2 using $2 * \pi * r * h$:

$$2 * \pi * (1 \times 10^{-4}\,\text{cm}) * (45 \times 10^{-4}\,\text{cm}) = 2.82 \times 10^{-6}\,\text{cm}^2$$

4.2 Calculating cGMP per cell

Our cGMP data was taken from[10], and it was given in total cGMP in pmoles for 10^8 cells. For our code, we want cGMP in terms of μM per cell.

$$\text{Total cGMPpmol} * \frac{1\,\mu\text{mol}}{1 \times 10^6\,\text{pmol}} * \frac{1\ \text{Total}}{10^8\text{cells}} * \frac{1}{\text{vol L}} = \frac{\text{cGMP}\ \mu\text{mol}}{\text{cell L}} = \frac{\text{cGMP}\mu\text{M}}{\text{cell}}$$

4.3 Cell Capacitance

For most cell lipid bilayers, $\frac{1\mu F}{cm^2}$ is a standard rate of capacitance.

Surface Area is $2.82 \times 10^{-6}\,\text{cm}^2$ Which results in:

$$\frac{1 \times 10^{-6}\,\text{F}}{\cancel{\text{cm}^2}} * 2.82 \times 10^{-6}\,\cancel{\text{cm}^2} = 2.8 \times 10^{-12}\,\text{F} = 2.8\,\text{pF}$$

4.4 Determining Ion Flux through Channels from the Faraday Constant and Cell Volume

Our Hodgkin Huxley ODEs will provide us with ion current in picoamps, and we know our cell volume. We can use the Faraday constant to determine the flux, as the units for F are $\frac{C}{\text{mole}} = \frac{A * s}{\text{mole}}$.

$$\text{ion flux } = \frac{1}{F * \text{ cell volume}} * \text{ ion current}$$

In terms of units

$$\frac{\text{mole}}{\text{vol} * s} = \frac{\text{mole}}{A * s * \text{vol}} * A$$

Therefore our ion flux ODE is in the form:

$$\frac{d \text{ ion conc.}}{dt} = \frac{1}{f} * \text{Ion current}$$

where f is a product of the Faraday constant and cell volume, and we will want the units to be:

$$\frac{\mu M}{\text{ms}} = \frac{1}{\text{f}}\text{pA}$$

therefore $\frac{1}{\text{f}}$ must be

$$\frac{\mu M}{\text{ms}} = \frac{\mu M}{\text{ms*pA}} * \text{pA}$$

Therefore f must be in $\frac{\text{ms*pA}}{\mu M} = \frac{\text{ms*pA* L}}{\mu\text{mole}}$ in order to convert the units observe, starting with:

$$\text{F * cell volume}$$

$$\frac{\text{A} * s}{\text{mole}} * \text{L}$$

$$\frac{\cancel{A} * \cancel{s}}{\cancel{\text{mole}}} * \text{L} * \frac{1 \cancel{\text{mole}}}{1 \times 10^6 \, \mu\text{mol}} * \frac{1 \times 10^{12} \, \text{pA}}{\cancel{A}} * \frac{1 \times 10^3 \, \text{ms}}{\cancel{s}} = \frac{\text{ms*pA* L}}{\mu\text{mole}} = \frac{\text{ms*pA}}{\mu M}$$

and we have that our conversion is:

$$f = \text{F* cell volume*} \frac{1}{1e6} * 1e12 * 1e3$$

This f can therefore be used to easily convert between concentration and current.

5 Parameter Estimation

The fmincon function in MATLAB was used for parameter estimation, this is a constrained nonlinear optimization technique. Constrained minimization is the problem of finding a vector x that is a local minimum to a scalar function $J(x)$, subject to the constraints allowable on x. As we know, on an order of magnitude, realistic values for our unknown parameters. We will let our parameters be the vector x and subject realistic constraints (upper and lower bounds on possible values for each variable). The trick is developing, and weighting, a cost function $J(x)$ which will result in a vector of parameters x minimizing the cost. Our cost will be from ideal data, therefore when x has minimal cost, that means they best fit the data.

The code works by repeatedly evaluating a cost function until x is minimized. In our case the cost function would be the difference between the ODE system evaluated with x parameters and real data

$$J(x) = (ode15s(x) - RealData)^2.$$

Once the cost function is minimized the fmincon fucntion will output the optimal ODE parameter vector x. In order to fit our unknown parameters, we were first interested in the the steady state case.

5.1 Steady State Case

In a steady state, with no Resact, the resting potential of the A. punctulata sperm is known to be -42mV [10]. The resting concentrations of intracellular ions were estimated from [1].

Steady State Voltage (VSS)=-42 mV

Steady State Ca^{2+} (CaSS)=0.2 nM

Steady State Na^{+} (NaSS)=30mM

Steady State K^{+} (KSS)=110mM

The first attempt at an error function J was to scale the voltage and ion concentrations and to just add their error. Our model used M data points.

$$J = \sum \left(\frac{1}{maxV} \left(V - VSS\right)^2 + \frac{1}{max[Ca^{2+}]} \left([Ca^{2+}] - CaSS\right)^2 + \frac{1}{max[Na^{+}]} \left([Na^{+}] - NaSS\right)^2 + \frac{1}{max[K^{+}]} \left([K^{+}] - KSS\right)^2 \right) / \left(4 * M\right) \tag{14}$$

The fmincon function did converge, though there was significant error,9 is the result of the parameter estimation. Observe how the voltage goes to zero. Through

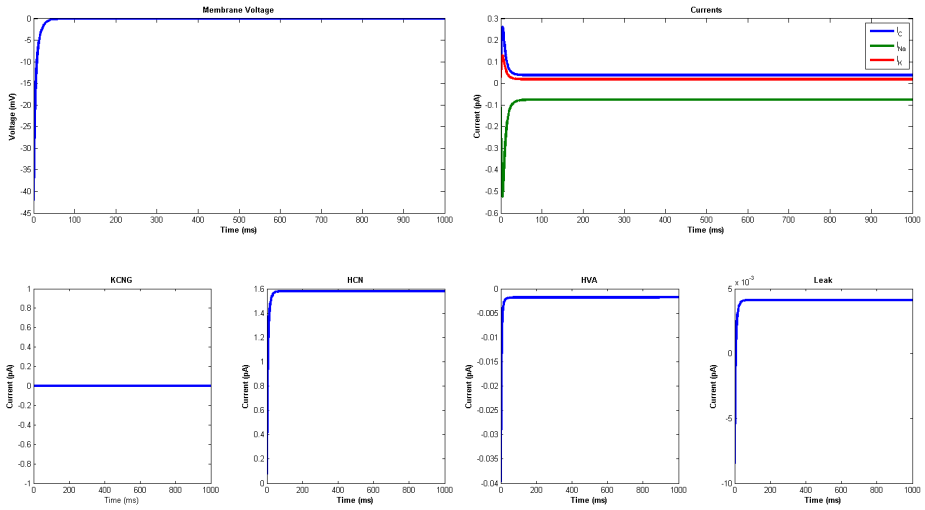

Figure 9: Steady state parameter estimation, currents. Membrane voltage is on the top left, NCKX currents are on the top right. All other ion channels are on the bottom. The large HCN current causes the to voltage crash to zero.

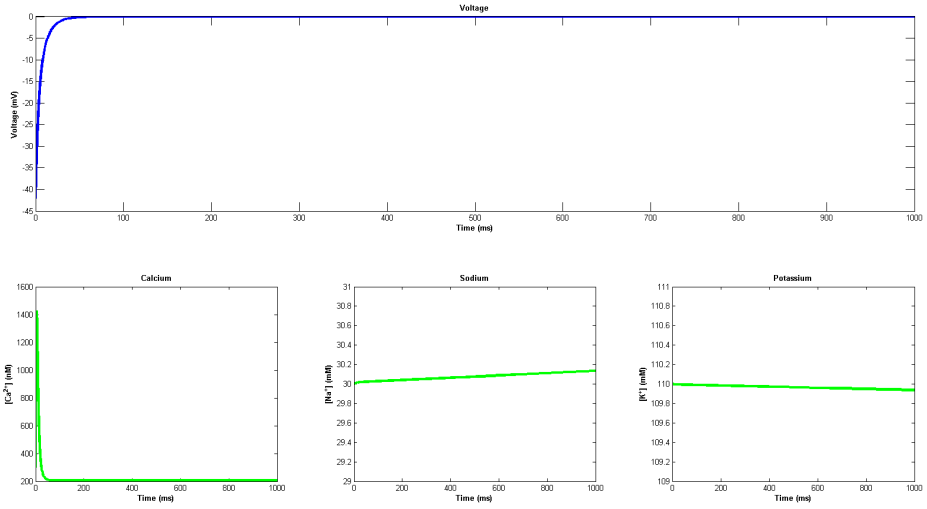

Figure 10: steady state parameter estimation, concentrations. Ca^{2+} has a large spike then crashes back down.

lots of trial and error, the optimal cost function was found to be

$$J = \frac{\sum \left((V - VSS)^2 + 100,000 \left([Ca^{2+}] - CaSS \right)^2 \right)}{2 * M}$$

Observe that the calcium had to be weighted heavily, and the other ion concentrations were not important. This cost function produced ideal steady state parameters, as all the currents and concentrations were realistic.

5.2 Testing the Steady State Parameters in the Presence of Resact

With optimal steady state values from the first parameter estimation, the model was tested by introducing cGMP data from Resact, this essentially turned on the KCNG channel. The model was stabilized for 1000ms before the Resact was introduced. The system hyperpolarized, yet failed to depolarize. Looking at the currents it is clear the NCKX exchanger increases productivity in response to

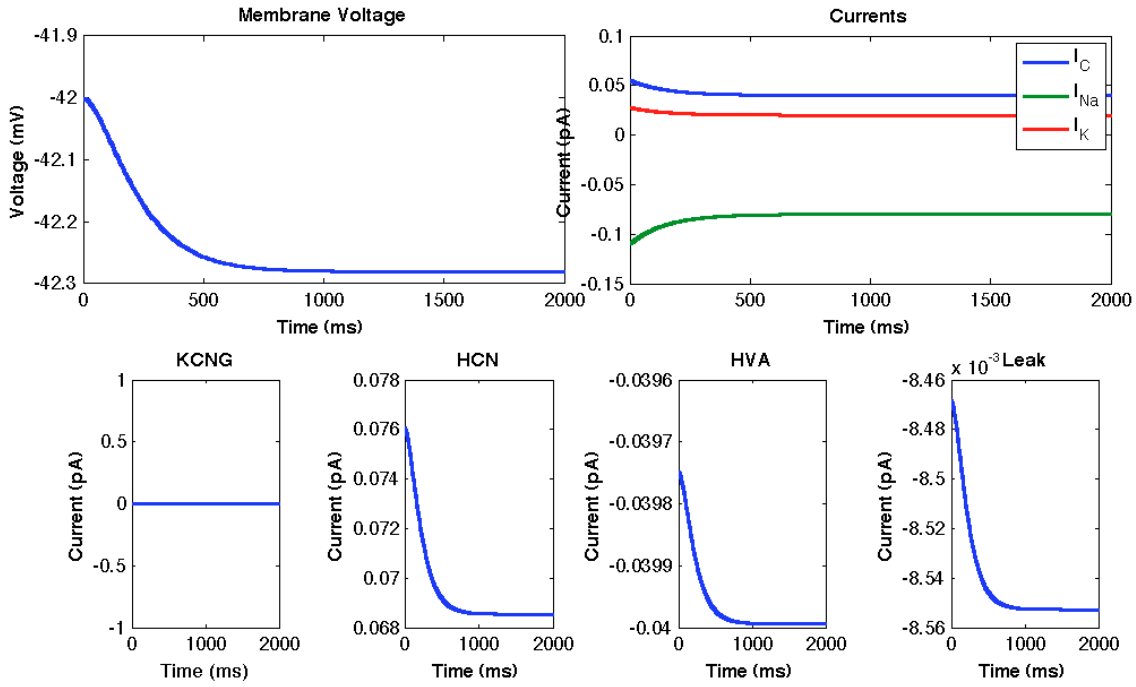

Figure 11: Optimal steady state parameter estimation, currents. Membrane voltage is on the top left, NCKX currents are on the top right. All other ion channels are on the bottom. Voltage is steady at an ideal level, with realistic stable currents from ion channels.

the hyperpolarization, causing Na^+ and K^+ to stabalize. Ca^{2+} increases, but not enough to cause depolarization. This indicates that the model may need a LVA Ca^{2+} channel. This behavior is seen clearly in Fig.13 and 14.

5.3 Active Case (Resact Present) Parameter Estimation

For the active case, where Resact is present, we had voltage and Ca^{2+} data from [17] at 25pM, which was their greatest concentration. For cGMP we had data from [10] at 0.25nM which was their smallest concentration, in pM the Resact for cGMP was 250pM, ten times greater than the Resact concentration for our voltage and calcium data. Though our best match up of data was off by a factor of 10 in regards to Resact concentration, this was a decent place to start. As the cGMP

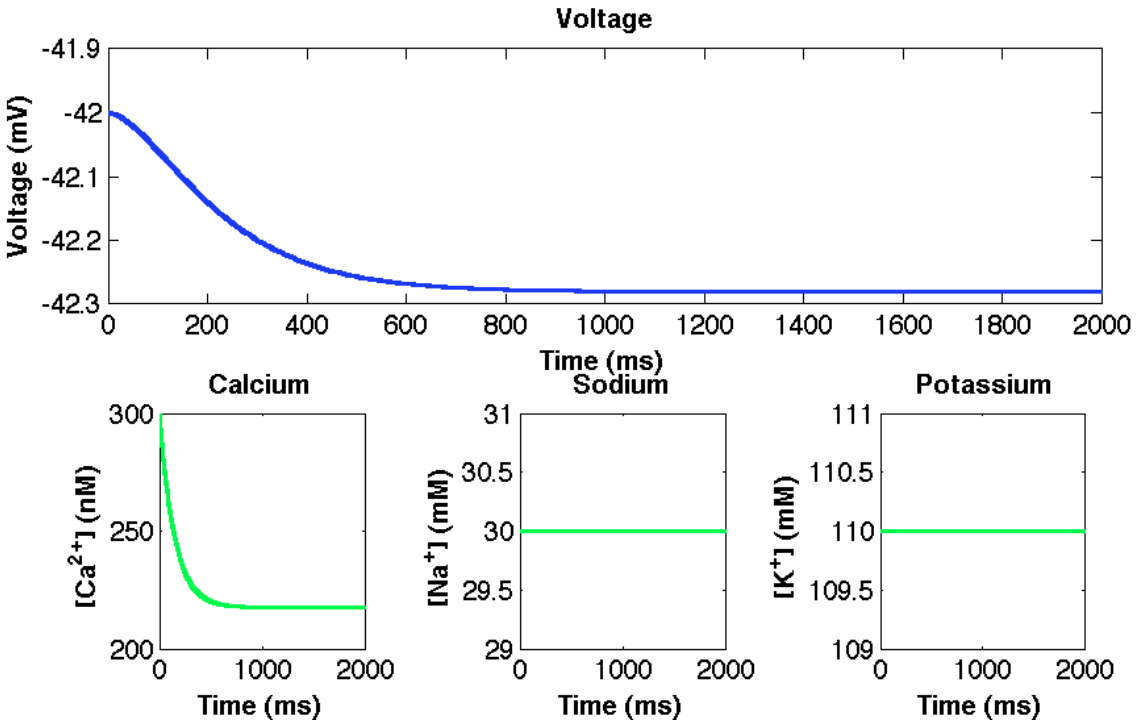

Figure 12: Optimal steady state parameter estimation, concentrations. All the ion concentrations match the target steady state concentrations and stabilize

data was only used to kick start the minf ODE, equation (5). The parameters from the steady state were used as an initial guess.

In order to persevere the steady state characteristics, the model was allowed to stabilize for 1000ms before the Resact was introduced. Once the Resact was introduced, voltage data (VData) and Ca^{2+} data (CaData) were interpolated from Fig. 8 [17] and used in equation (6).

Our error function was simply:

For time zero to 1000ms

$$J = \sum \left((V - VSS)^2 - \left([Ca^{2+}] - CaSS \right)^2 \right) / (2 * M) \tag{15}$$

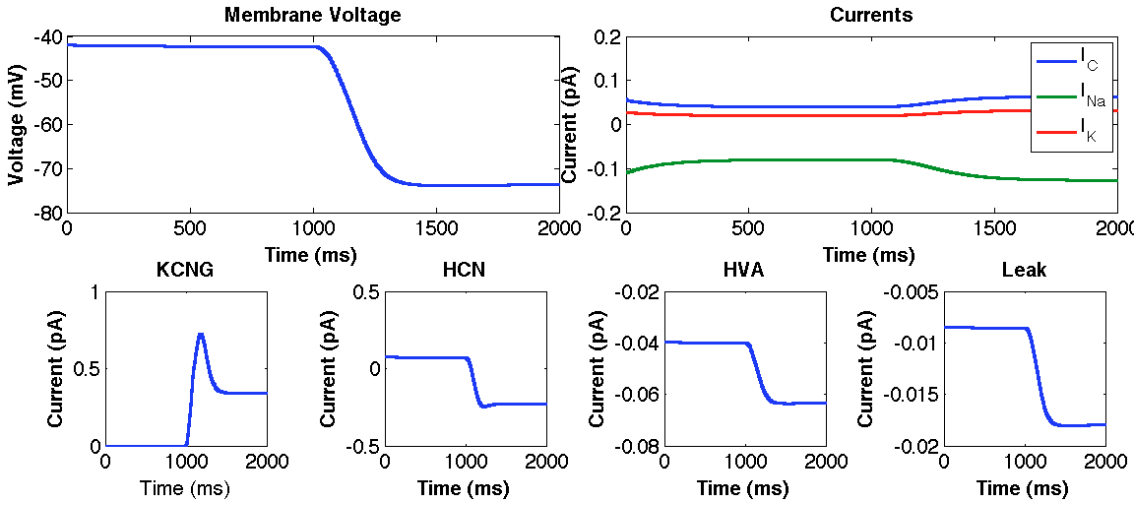

Figure 13: Active (with cGMP) optimized steady state parameters, currents. Membrane voltage is on the top left, NCKX currents are on the top right. All other ion channels are on the bottom. The system hyperpolarizes, yet fails to depolarize.

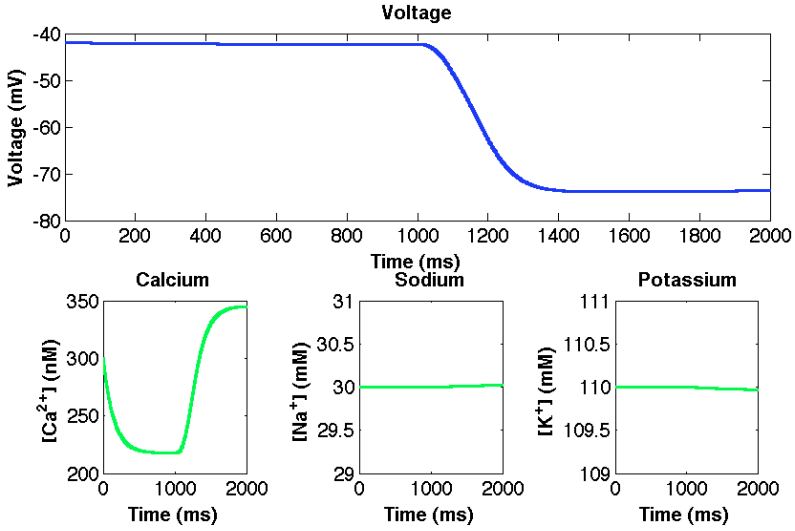

Figure 14: Active (with cGMP) optimized steady state parameters, concentration. The calcium concentration increases during hyperpolarization, yet the system fails to depolarize. Sodium and potassium currents remain constant, as the NCKX exchanger begins to increase. This indicates that another calcium channel (LVA) may be necessary in the model.

For time 1000ms to the end of the real Data

$$J = \sum \Big((V - VData)^2 - \\ \left([Ca^{2+}] - CaData \right)^2) \Big) / (2 * M) \tag{16}$$

Many other weight functions were attempted, along with different permutations

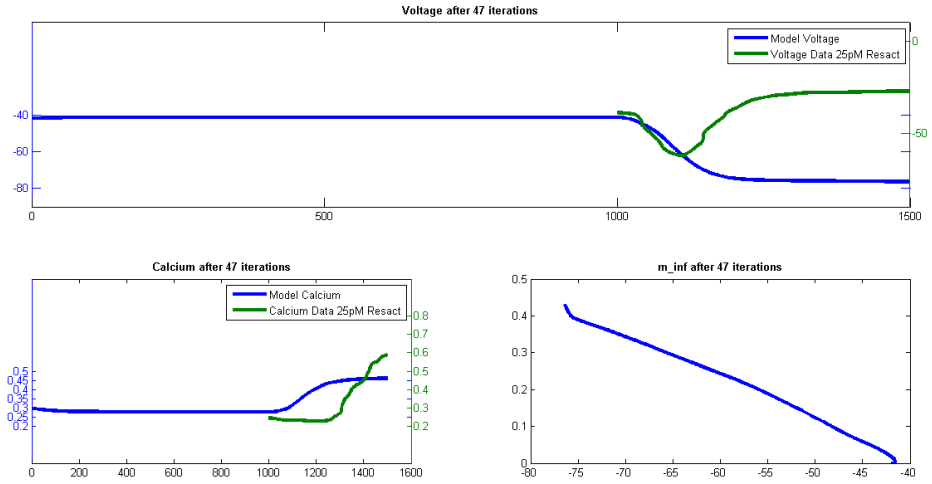

Figure 15: Parameter Estimation using Real data for Calcium and Voltage in 25pM of Resact and cGMP data from .25nM of Resact. The voltage hyperpolarization is effectively captured, though the cell never depolarizes. The shift in calcium is also captured, though the exact behavior of the curve is poorly replicated.

of parameters to be estimated, none of the error functions would found to converge a small error.

6 Discussion

This model does an effective job in replicating the resting state of the sperm cell (when there is no Resact). However, the heavy weighting on the behavior of the Ca^{2+} indicates this model was not ideal. Perhaps separating the calcium channel into an HVA and LVA channel would provide this model with enough flexibility to depolarize properly.

References

[1] LU Aguilera, BE Galindo, D Sanchez, and M Santillan. What is the core oscillator in the speract activated pathway of the Strongylocentrotus purpuratus sperm flagellum? *Biophys J*, 102:2481–2488, 2012.

[2] L Alvarez, L Dai, BM Friedrich, ND Kashikar, I Gregor, R Pascal, and UB Kaupp. The rate of change in Ca^{2+} concentration controls sperm chemotaxis. *J Cell Biol*, 96(5):653–663, 2012.

[3] F Buchholtz, J Golowasch, IR Epstein, and E Marder. Mathematical model of an identified stomatogastric ganglion neuron. *J Neurophys*, 67(2):332–340, 1992.

[4] D Duhaney. Mathematical model of chemotactic signaling in sea urchin sperm. MQP, 2013.

[5] BE Galindo, JL la Vega-Beltra, P Labarca, VC Vacquier, and A Darszon. Sptetra KCNG: A novel cyclic nucleotide gated K^+ channel. *Biochem Biophys Res Comm*, 354:668–675, 2007.

[6] AL Hodgkin and AF Huxley. A quantitative description of membrane current and its application to conduction and excitation in nerve. *J Physiol*, 117:500–544, 1952.

[7] D Kase and K Imoto. The role of HCN channels onmembrane excitability in the nervous system. *J Signal Transduction*, pages 619747–1–11, 2012.

[8] ND Kashikar, L Alvarez, R Seifert, I Gregor, O Jackle, M Bayermann, R Kraue, and UB Kaupp. Temporal sampling, resetting, and adaptation orchestrate gradient sensing in sperm. *J Cell Biol*, 198(6):1075–1091, 2012.

[9] UB Kaupp, E Hildebrand, and I Weyand. Sperm chemotaxis in marine invertebrates–molecules and mechanisms. *J Cellular Physiol*, 208:487–494, 2006.

[10] UB Kaupp, ND Kashikar, and I Weyand. Mechanisms of sperm chemotaxis. *Annu Rev Physiol*, 70:93–117, 2008.

[11] Bryn Mawr. Hodgkin huxley equations, 2014.

[12] Tokyo Institute of Technology. Equivalent circuit of neuron, 2014.

[13] University of Tokyo. Mechanism of sperm chemotaxis: How are spermatozoa guided to eggs?, 2014.

[14] D Sanchez, P Labarca, and A Darszon. Sea urchin sperm cation selective channels directly modulated by cAMP. *FEBS Letters*, 503:111–115, 2001.

[15] KS Shin, C Maertens, C Proenza, BS Rothberg, and G Yellen. Inactivation in HCN channels results from reclosure of the activation gate: desensitization to voltage. *Neuron*, 41:737–44, 2004.

[16] D Sochivko, A Pereverzev, N Smyth, C Gissel, T Schneider, and H Beck. The CaV2.3 Ca^{2+} channel subunit contributes to R-type Ca^{2+} currents in murine hippocampal and neocortical neurones. *J Phys*, 542:699–710, 2002.

[17] K Strunker, I Weyand, W Bonigk, Q Van, A Loogen, and et al. A K^{+}-selective cGMP-gated ion channel controls chemosensation of sperm. *Nat Cell Biol*, 8:109–17, 2006.

[18] YS Su and VD Vacquier. A flagellar K^{+}-dependent na!!ca2! exchanger keeps Ca^{2+} low in sea urchin spermatozoa. *PNAS*, 99:6743–6748, 2002.

[19] SS Suarez. Control of hyperactivation in sperm. *Hum Reprod Update*, 14:647–658, 2008.

[20] SS Suarez. How do sperm get to the egg? bioengineering expertise needed! *Exp Mech*, 50:1267–1274, 2010.

[21] SS Suarez and AA Pacey. Sperm transport in the female reproductive tract. *Humn Reprod Update*, 12:23–37, 2006.

[22] Wikepedia. Sperm, 2013.

[23] CD Wood, A Darszon, and M Whitaker. Speract induces calcium oscillations in the sperm tail. *J Cell Biol*, 161:89–101, 2003.

[24] CD Wood, T Nishigaki, T Furuta, SA Baba, and A Darszon. Real-time analysis of the role of ca^{2+} in flagellar movement and motility in single sea urchin sperm. *J Cell Biol*, 169:725–731, 2005.

[25] CD Wood, T Nishigaki, Y Tatsu, N Yumoto, SA Baba, and et al. Altering the speract-induced ion permeability changes that generate flagellar ca^{2+} spikes regulates their kinetics and sea urchin sperm motility. *Dev Biol*, 306:525–37, 2007.